Chapter 2

DIAGNOSTIC IMAGING

State-of-the-art and Recent Advances

Falko Busse
Philips Research, Hamburg, Germany

Abstract: Medical imaging is the heart of many diagnostic and therapeutic procedures. Starting from the discovery of X-rays in 1895, a number of imaging modalities were invented and later established in clinical practice. Initially these imaging modalities (except PET and SPECT, which target metabolic processes) were aimed to visualize non-invasively anatomical details from within the body. With the improvement of imaging agents, computing power and imaging technology increasingly information about organ function and even metabolism can be measured and used in the clinical decision process. However, all established imaging modalities have strengths and weaknesses. Therefore, a strong trend exists to combine complementary information from different imaging modalities, either through system integration or software fusion. PET-CT is an impressive manifestation of this trend. In addition, work continues to explore novel imaging techniques with the aim to develop new modalities. These would help to close remaining clinical gaps with imaging as the enabler.

Keywords: Imaging modalities, hybrid imaging, functional imaging, molecular imaging, X-ray, CT, PET, SPECT, MR, ultrasound, optical imaging, photoacoustic tomography, magnetic particle imaging

1. INTRODUCTION

Radiology began as a medical sub-specialty in the first decade of the 1900's after the discovery of X-rays. The development of radiology grew at a moderate pace until World War II. Extensive use of X-ray imaging during the second world war, and the advent of the digital computer and new imaging modalities like ultrasound, computed tomography, magnetic resonance imaging and nuclear imaging have combined to create an

G. Spekowius and T. Wendler (Eds.), Advances in Healthcare Technology, 15-34.

explosion of diagnostic imaging techniques in the past 25 years. Some of the major milestones in the development of medical imaging technology are summarized in Table 2-1.

Table 2-1. Milestones in medical diagnostic imaging.

Date	Innovation
1895	Wilhelm Conrad Roentgen discovers X-rays. He also produces the first X-ray image of the human body (his wife's hand).
1953	First real-time Ultrasound device built by John Julian Wild and John Reid[1].
1963	Tomographic SPECT reconstruction by David Kuhl and Roy Edwards[2].
1972	CT scanning is invented by Sir Godfrey Hounsfield and Allan Cormack[3].
1974	Clinical PET (Positron Emission Tomography) developed at the University of Washington[4].
1980	First MR imaging of the brain on a clinical patient. MR was developed by Paul Lauterbur and Peter Mansfield[5,6].

Today, imaging systems reveal every organ and lay bare every pathology. They show us three-dimensional, full-color pictures of the beating heart and cross-sectional slices of the abdomen. We can see blood flowing through our arteries, water traveling along nerve fibers, cells dying in a tumor, antibodies battling infection, and, strangest of all, emotions such as fear and love arising in the brain. These devices even analyze the images they produce; they identify malignancies, count plaque deposits in arteries, measure bone loss, and calculate the heart's pumping capacity. They also assist surgeons, tracking the positions of their instruments in real time and letting them know what their scalpels are about to cut into.

The increasing importance of medical imaging in diagnosis and treatment planning is demonstrated by the fact that, in addition to X-ray (W. C. Roentgen), two imaging technologies have been awarded with the Nobel Prize. Allan M. Cormack and Godfrey N. Hounsfield received the prize "for the development of computer assisted tomography" in 1979, and Paul C. Lauterbur and Peter Mansfield "for their discoveries concerning magnetic resonance imaging" in 2003.

2. TECHNOLOGY TRENDS

The field of medical imaging developed along a few major trends, especially since the mid 1970's. These high level trends can be summarized in a short bullet list:

- Towards fully integrated solid state detectors.
- Towards 3D image matrix.

- Speed-up of acquisition towards 4D (3D+T) images.
- From anatomical to functional to molecular imaging.

The main driver behind this development (or better called enabler) is the exponential growth in performance of silicon devices, both in the area of digital logic as well as processing units. This growth can well observed in e.g. Moore's law[7], which is depicted in Figure 2-1.

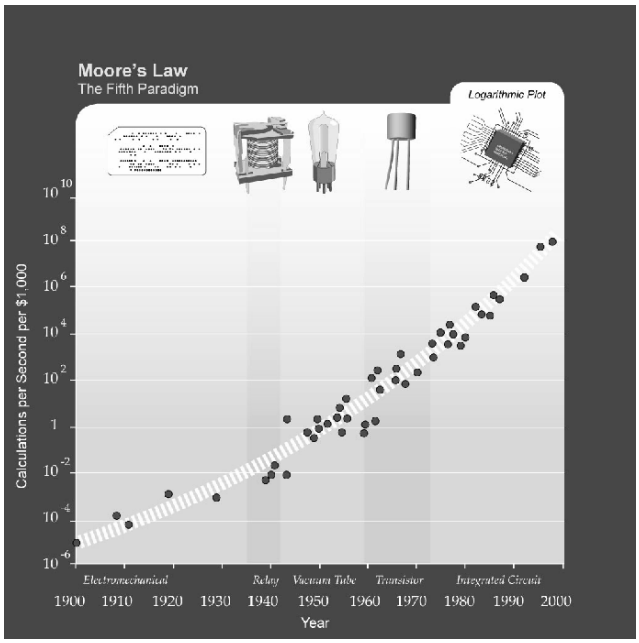

Figure 2-1. Moore's law using Intel processors as example (image courtesy of Intel Corp.).

The general trends in imaging technology, as described above, drive the development of the established imaging modalities. Although the onset and the speed of these developments vary between imaging technologies, the trends can be observed generally throughout the modalities. In the following sections the impact of the trends on improvements in technology will be discussed.

2.1 X-ray

The use of X-rays for diagnostic imaging started shortly after Wilhelm Konrad Roentgen's discovery in 1895. Since X-rays penetrate solid objects,

but are slightly attenuated by them, the picture resulting from the exposure reveals the internal structure of the human body. X-ray imaging was and is still used in two applications fields: Radiography and fluoroscopy.

Imaging technology for radiography evolved from plain X-ray film and screen-film combinations to cassette-based computed radiography, introduced 1983 by Fuji[8]. This technology enabled the step of X-ray imaging into the digital domain. However, the conversion from X-rays into digital signals is not performed directly, but requires an intermediate (analog) storage step in photostimulable phosphors[9]. Only recently, a new technology based on large area amorphous silicon plates has been introduced to the market, which converts the incoming X-rays either via a photoconductor layer[10,11] or via a scintillator/photodiode combination[12,13] directly into digital signals. This technology is explained in detail in Chapter 4.

Fluoroscopic imaging initially relied on fluorescent screens. But since doctors then would stare directly into the X-ray beam, such screens were quickly replaced by image intensifiers / television camera combinations after 1954, the year of introduction. Figure 2-2 shows one of the first commercial image intensifier systems from the year 1954.

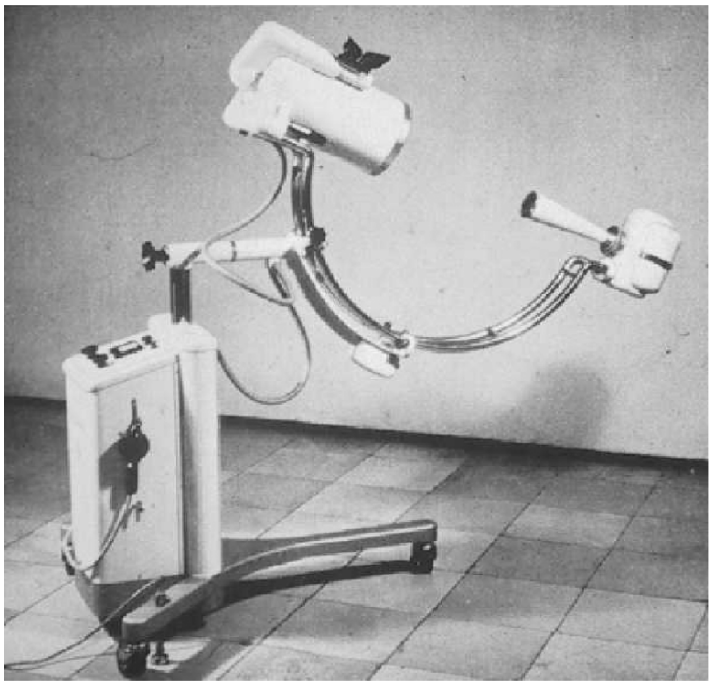

Figure 2-2. The first commercial surgical image intensifier system (BV 20) from Philips.

After the introduction of radiographic detectors based on amorphous silicon technology end of the 1990s, it was only a question of time when the more challenging implementation of fluoroscopic detectors on the same technology would be introduced[14,15]. Due to the advantages of a much more compact design and distortion free images at higher contrast resolution, these detectors have become the mainstream imaging technology in X-ray.

The next technology change already appears at the horizon. Detectors based on large area CMOS technology are available in the early prototype stage for proof-of-concept[16]. The anticipated advantages will be higher spatial resolution, higher readout speed for functional and 3D imaging at potentially lower cost of goods.

The application range of X-ray fluoroscopy spans from classical radiology, interventional radiology, surgery to cardiovascular interventions. As a very successful procedure 3-dimensional rotational X-ray imaging has been introduced in the 1990s[17], expanding the application space into volumetric anatomy and function (compare Chapter 5). There is significant research effort spent to replace the diagnostic interventional procedures performed with X-rays by MR and CT, because of their non-invasive nature.

However, with respect to clinical outcome X-ray is still the gold standard. At the same time, X-ray leverages its real-time capabilities and its high spatial resolution to expand into new and more complex therapeutic applications like integrated navigation (more details in Chapter 11) and cancer treatment (see Chapter 10).

2.2 Computed tomography (CT)

Computed tomography acquires a large number of projection X-ray images from a patient from various angles, usually by rotating X-ray source and detector around the patient. The collection of projection images is then translated into a 3-dimensional volume of linear attenuation coefficients (usually displayed relative to water). Using the first commercial CT systems, scanning just one slice of a human brain took nine hours, with subsequent reconstruction of 2.5 hours. The resulting slice image had a matrix of 80^2 pixels and a contrast resolution of 8 Bit. A picture of one of these first CT systems is shown in Figure 2-3.

Modern CT systems acquire and reconstruct image matrices up to 1024^2 pixels, at a rate of 40 slices per second (for a 512^2 matrix). The contrast resolution of these images is 18 Bit. Reconstruction can be synchronized to breathing and/or cardiac motion, in order to compensate for motion artifacts.

This enormous gain in acquisition speed has been achieved by faster rotation of the gantry (currently at 0.4 seconds per rotation) and by adding more and more detector lines for parallel image acquisition. Current state-of

the-art are systems use 64 of such detector lines. In order to avoid that the costs of such systems explode, new paradigms in detector technology have to be pursued, as described in Chapter 4.

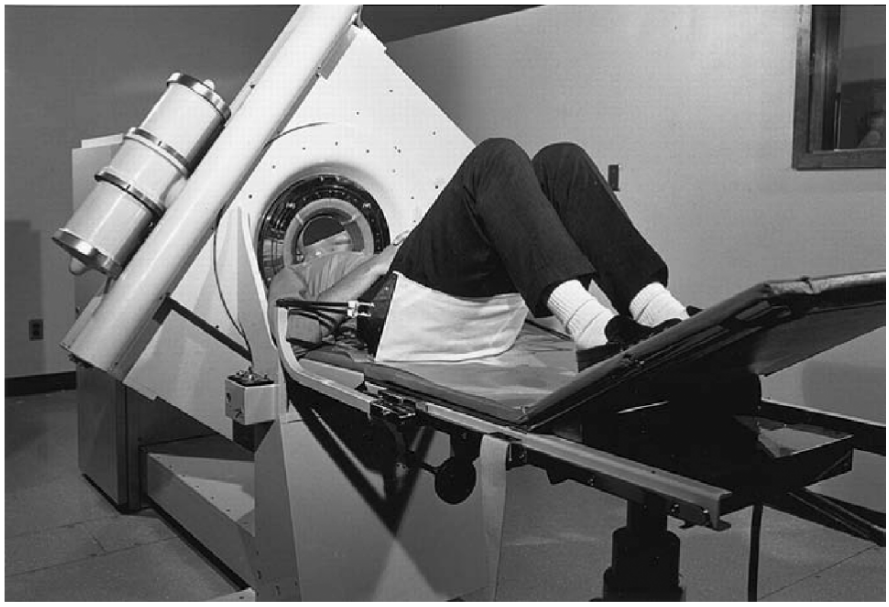

Figure 2-3. Original head CT scanner from EMI (installed at Mayo Clinic, Rochester, Minn.). Image courtesy of the RSNA.

Increasing the detection area generates also challenges to the technology in all other aspects of the system. The bandwidth of the slip ring, through which the data has to be transmitted from the rotating detector to the static part of the gantry, has to multiply in correspondence with the number of detector lines. The reconstruction problem changes drastically, from a fan beam geometry to a cone beam geometry, for which only recently a mathematical approach for an exact solution has been found[18]. A detailed discussion of the state-of-the-art in reconstruction technology is given in Chapter 3.

2.3 Positron emission tomography (PET)

PET images the 3-dimensional distribution of a tracer, which has been injected into the human (or animal) body. The tracer is labeled with a positron-emitting radioisotope. Once emitted, the positrons travel a short distance (0.2 mm for ^{18}F, 0.3 mm for ^{11}C, 0.4 mm for ^{15}O, 0.8 mm for ^{82}Rb,

all FWHM), before they annihilate with an electron into two photons of 511 keV that are emitted almost exactly in opposite directions. These two photons are then detected in coincidence.

The fundamental building blocks of PET imaging has not changed over the first 30 years after introduction of the technology. PET detectors consist of a ring shaped layer of scintillation crystals, which are glued to a light guide, and a layer of photomultiplier tubes attached to the outside of the light guide. The scintillator absorbs the incoming γ-rays of 511keV energy and converts them into optical signals. The light guide then spreads the optical photons on several photomultiplier tubes, which allows for an exact reconstruction of the crystal (pixel) which was hit. A more detailed description of PET technology is given in Chapter 8.

Nevertheless, there was significant performance improvement of PET systems over time. This is due to improvements in key components like the scintillation material. The characteristics of the scintillator determine critically the PET imaging performance. Important parameters are especially the detection efficiency, energy resolution, time resolution, emission wavelength, mechanical and hydroscopic properties. Table 2-2 gives an overview of scintillator materials commonly used for PET (adapted from [19]).

Table 2-2. Physical properties of scintillator material commonly used for PET.

Scintillator material	Attenuation length [mm]	Light outout [ph/MeV]	Decay time [ns]	Emission wavelength [nm]	Hydroscopic
BGO	10.4	9000	300	480	No
LSO	11.4	30000	40	420	No
NaI:Tl	29.1	41000	230	410	Yes
CsI:Tl	22.9	66000	900	550	Slightly
GSO	14.1	8000	60	440	No
LuAP	10.5	12000	18	365	No
LaBr3	21.3	61000	35	358	No
LYSO	11.2	32000	48	420	No
LuAG	13.4	5606		510	No

For high intrinsic efficiency, scintillator materials should have both a high effective atomic number Z_{eff} and a high density. The energy (and spatial) resolution is associated with the light yield from the scintillator, since the magnitude of the fluorescent light yield will reduce the statistical spread in accordance with $(n_{ph})^{-1/2}$.

Whereas early PET scanners relied on NaI:Tl and Cesium Fluoride scintillators[20-22], modern PET systems are based on BGO[23], GSO[24] and LSO[25] crystals. Actual developments in the field of new detection technologies are directed towards the use of new cerium doped crystals, the use of layered crystals and other schemes for depth-of-interaction (DOI) determination, and a renewed interest in old technologies such as time-of-

flight (TOF) PET[26], taking advantage of excellent timing resolution of new scintillators, along[27]. It appears that cerium doped lutetium orthosilicate (LSO:Ce), lutetium yttrium orthosilicate (LYSO:Ce) and cerium doped lanthanum bromide ($LaBr_3$:Ce), are the most promising candidates[28].

Recent developments in photodetectors for medical applications should enable efficient collection of the light emanating from the scintillation crystals[29,30]. The design of high resolution imaging devices imposes some additional constraints with respect to the necessity for compact arrays of photodetectors; in turn, this has stimulated the development and use of multichannel position-sensitive photomultiplier tubes (PS-PMT's), Silicon p-i-n photodiodes (PDs) and avalanche photodiodes (APDs)[31,32]. Solid-state photodiodes exhibit many advantages compared to conventional PMT's. They are relatively small, operate at much smaller voltage, and more importantly, and exhibit higher quantum efficiencies. Furthermore, photo-diodes are insensitive to axial and transversal strong magnetic fields and therefore, have the potential to be operated within MRI systems. By using this technology, the sensitive area of the detector could be read out more efficiently.

2.4 Single photon emission tomography (SPECT)

Similar to PET, SPECT images a radioactively labeled tracer. However, the labels in SPECT are γ-emitters, which emit in an energy range between 69 keV (^{201}Tl), and 365 keV (^{131}I), Most commonly used is ^{99m}Tc due to its moderate emission energy of 140 keV, its convenient decay time (6 hours) and its availability in generators.

Shortly after Hal Anger[33] developed the concept of a detector based on a single NaI crystal and an array of photomultiplier tubes, first tomographic images were produced[2]. The detection concept, which includes also a collimator in front of the scintillation crystal for selecting the projection, is still widely used in today's commercial systems.

The main innovations in SPECT therefore occurred in the areas of data acquisition, reconstruction[34] and image analysis.

Nevertheless, there are still attempts to overcome the drawbacks of the Anger camera, namely the reduced sensitivity and spatial resolution due to the collimator, by the means of new imaging technology. A technology that is potentially close to market introduction is the solid-state detector based on the direct conversion material CZT (see Chapter 4 for further information). Solid-state detectors should have intrinsically a better energy resolution, which would lead to lower scatter background. As a consequence, simultaneous dual isotope imaging might be achievable, which would

drastically improve workflow of some clinical procedure like stress/rest imaging for cardiac perfusion measurement.

SPECT cameras based on CZT would probably exhibit an improved spatial resolution, but would not solve the intrinsic problem of the reduced sensitivity. One approach to eliminate the collimation at least in one dimension is based on slat detectors with a Slit collimator[35]. The detector together with the collimator would then rotate to achieve some collimation in the second dimension. Such systems exist is a prototype stage, but are not yet commercially available.

Already 1977 the concept of the Compton camera was proposed[36], which tries to replace the mechanical collimation by an electronic one, and thus boost the sensitivity of the detector. This concept has, however, still some significant technical challenges to solve, e.g. to achieve the required detector specifications at reasonable costs and to solve the reconstruction problem.

2.5 Magnetic resonance imaging (MR)

MRI is well recognized as a commonly used medical imaging modality. In spite of its significant growth over the last two decades, technical and application development continues.

Historic developments in image acquisition approaches are summarized in Table 2-3, where the periods of evolution are apportioned into approximately five- to ten-year-long intervals.

Table 2-3. Evolution of MR image acquisition approaches.

Time	Acquisition strategy
Mid 1980s	Identical magnetization level for all phase encodings. Identical pulse sequence used for all phase encodings (e.g. FLASH).
Late 1980s	Efficient use of decaying transverse magnetization (e.g. RARE, FSE, TSE). Allowance for different magnetization levels for different phase encodings. Non-rectilinear k-space trajectories.
Late 1990	Allowance for different pulse sequences for different phase encodings. Synthesis of required encodings from sparsely sampled measured set (e.g. SENSE, SMASH).

Two techniques have been developed for the synthesis of data at 'missing' values: Sensitivity encoding (SENSE[37]) and simultaneous acquisition of spatial harmonics (SMASH[38]). Both methods are similar in that an array of receiver coils is used, rather than a single coil. Further, both techniques use the differential response of individual coil elements across the field of view as the basis for generating the missing phase encodings. It has also recently been shown that the SENSE concept can be adapted for the parallel transmission of multi-dimensional RF pulses[39].

One of the driving forces behind MR developments is the need to accommodate increasing image reconstruction demands. A second driver is the emergence of specific research-based methods developed several years ago and the desire to make them more practical. One example of this is functional (f) neuro MRI. With this method a sequence of images of the brain is rapidly acquired over 1 to 2 min while the subject is performing some physical or mental task. A third driving factor is the identification of specific applications in which interactive MR imaging with real-time control is essential. One example of this is the use of real-time navigator echoes to guide the acquisition of data that can be subject to motion degradation (e.g. respiratory motion during a cardiac scan). Another example for which interactive imaging is essential is tracking of catheters and guidewires during interventions.

An example of a procedure that found its way from a research tool into clinical application is diffusion-weighted MR imaging. Perhaps the first clinical application of DWI was reported 1996, showing diffusion deficit in the presence of a stroke[40]. Applications of DWI have developed also into MR tractography, which connects pixels in relation to the anisotropy of the diffusion tensor. The technique can possibly be used to assess white matter tracts as part of neurosurgical planning.

3. HYBRID IMAGING MODALITIES

Historically, in each major disease category one medical imaging modality of choice has been established as gold standard. Driven by the growing acceptance (reimbursement) of functional and metabolic imaging modalities like PET, this paradigm has changed towards the improvement of sensitivity and specificity of diagnostic imaging also by means of combining information from two (or more) modalities.

Hybrid systems can be realized with different degrees of integration. The architecture of such systems may range from an integrated backend only (with high-speed data exchange and image fusion functionality), over in-line systems that share mechanical components like the patient table, to fully integrated combinations. The choice of the architecture is mainly determined by the clinical value that is provided by the hybrid system, and technical boundary conditions.

Generally speaking, higher degrees of integration will reduce registration errors and will improve workflow for specific applications. In addition, it will allow for the simultaneous imaging with both modalities, which is an enabler for certain diagnostic applications. On the other hand, higher degrees of integration may lead to a reduced flexibility and patient scheduling.

Making an attempt to categorize the field of hybrid imaging modalities, the main driver behind hybrid systems for *diagnostic imaging* purposes has been the improved diagnostic power from combining functional / metabolic and anatomical information. Imaging in the context of molecular therapeutics will also give rise to a large demand for hybrid systems in the area of *therapy response assessment*. Applications of hybrid imaging systems in *image-guided treatment* have been in clinical trials much longer than those for diagnostic imaging. Examples are the integration of X-Ray C-arm systems (also in hybrid combination with CT or MR) with intra-vascular treatment devices, and of MR with high-intensity focused ultrasound (HIFU), and the increasing integration of real-time 3D Ultrasound in interventional treatment.

3.1 Hybrid diagnostic imaging

For PET, with its high sensitivity but low spatial resolution, it was obvious that an anatomical reference image would greatly enhance its value for diagnosis and therapy planning in oncology applications. After some initial debate about whether the images from two separate modalities could simply be fused by suitable image processing algorithms, the market simply decided for *integrated* PET-CT combinations. First systems were introduced in 2001, and today the market for standalone PET systems has virtually disappeared. And even though the CT part of the hybrid combination is running idle ca. 90% of the time during a hybrid exam, the market keeps replacing CT scanners with PET-CT hybrid systems.

Although today still 90% of all PET examinations are performed with ^{18}F-FDG, there is a large research effort spent both in academia as well as in industry to develop and commercialize new imaging agents for PET (compare Chapter 18). These agents will potentially be targeted to metabolic processes or receptors that are very specific to certain diseases. As a consequence, the level of anatomical information in PET images will tend to decrease further, which increases the need for an anatomical reference by a second modality.

With respect to agents, clinical SPECT is further advanced. A number of agents are approved, both for oncology and cardiology applications, and many more are in clinical trials. Some of these agents are targeting specific metabolic processes, and can therefore be called molecular agents already. Therefore, it was a natural step that SPECT-CT was introduced 2004 as the second hybrid modality into the market. Clinical applications for these systems will be both in cardiology (diagnosis and risk stratification of coronary artery disease) and in oncology (diagnosis, staging and follow-up).

As a potential future opportunity for hybrid diagnostic modalities, combinations of MR with either PET or SPECT are considered. These combinations are currently in the research phase, with respect to technology as well as to clinical applications. The main technical challenge for an integrated system is the sensitivity of the photo-multiplier tube, which is a critical component in today's PET and SPECT detectors, to the magnetic field of the MR. Recent successes in replacing the PMTs by Avalanche photodiodes may open a route for a technical realization. Nevertheless, experience from the PET-CT development tells that both modalities in hybrid systems need to have state-of-the-art performance. Such performance still needs to be demonstrated in the case of Avalanche photodiodes, especially if the PET technology moves towards time-of-flight.

3.2 Hybrid imaging in image-guided treatment

Applications of hybrid imaging systems in image-guided treatment have been addressed in clinical trials much earlier than those for diagnostic imaging. However, they have largely remained in the experimental stage and aimed at very specific treatment procedures. They are also less standardized, and have thus not led to spectacular market successes so far. Examples are combinations of X-Ray C-Arm systems with CT and MR (see Chapters 9 and 10), or combinations of optical (microscopic and endoscopic) imaging with MR and Ultrasound. In Cardiology, the increasing attention to detecting vulnerable plaque in coronary arteries and to the treatment of cardiac arrhythmia in the Electrophysiology Lab has stimulated a renewed discussion about the combination of intra-vascular (mainly Ultrasound and Optical) imaging with fluoroscopic modalities like X-Ray (see Chapter 11). Increasingly, also CT and MR are considered for EP guidance, as the 4D fluoroscopic capabilities of these modalities improve. A significant role might evolve for real-time 3D Ultrasound, as the fastest and cheapest '4D-imaging' modality, which is increasingly considered for interventional guidance in a number of application areas (see Chapter 7 for further reading).

3.3 Hybrid imaging to assess therapy response

Apart from the areas mentioned above, there are increasing clinical research efforts in hybrid systems for planning and delivery of non-invasive therapy, in order to provide closed loop solutions in which imaging derived information about the therapeutic procedure is used to control the delivery devices. One example is radiation therapy of tumors using linear accelerators, which are equipped with X-Ray imaging systems for organ motion tracking

and corresponding collimation control (see details in Chapter 13). Another oncology procedure is based on non-invasive High-Intensity Focused Ultrasound (HIFU) ablation devices, which are integrated into MR systems. In this combination, the MR system is used for targeting control of the ultrasound focus volume and for monitoring of the resulting 3D temperature distribution. A detailed overview on this technique is given in Chapter 12.

4. NOVEL IMAGING TECHNOLOGIES

Besides the imaging modalities that are already established in clinical practice, there are a number of imaging principles currently in the research phase with the aim to develop them into clinically useful tools for imaging in humans.

Since more than ten years, considerable interest is devoted to optical imaging. Optical imaging is today routinely used only in pre-clinical imaging of small animals. Advancing optical techniques to humans promises high sensitivity without the use of ionizing radiation. However, significant technical challenges have to be overcome, since optical photons are strongly scattered and absorbed by human tissue.

The technical challenges of optical imaging can be somewhat reduced through a technique called photoacoustic tomography. In this concept the optical photons are used only to deposit energy at the location of the imaging agent, and then the resulting temperature increase is imaged with Ultrasound.

Finally, another method to detect small concentrations of an imaging agent is the utilization of the magnetic properties of the imaging agent. Such a technique, called Magnetic Particle Imaging, has recently been proposed.

4.1 Optical imaging

Visual light and near-infrared light offer the opportunity to image biological tissue, even though the predominant interaction processes are scattering and absorption. In the near-infrared window of low water absorption, tomographic optical imaging might be possible. However, due to the strong scattering and absorption of photons, there seems to be a limit for the size of body parts at approximately 10 cm in diameter.

Recently, the emphasis of research in medical imaging with diffuse light has moved away from the pursuit of high spatial resolution and towards functional imaging. It is widely appreciated that diffuse optical imaging can never compete in terms of spatial resolution with anatomical imaging

techniques, but offers several distinct advantages in terms of sensitivity to functional changes, safety, cost and use at the bedside.

Three different technology approaches for diffuse optical tomography can be identified: Continuous wave, time domain and frequency domain. Philips Research pioneered the continuous wave approach through the development of a breast imaging system[41] (the prototype is shown in Figure 2-4). A comprehensive comparison of the different approaches as well as a description of the state-of-art of the technology and the clinical applications has been published by Gibson, Hebden and Arrige[42].

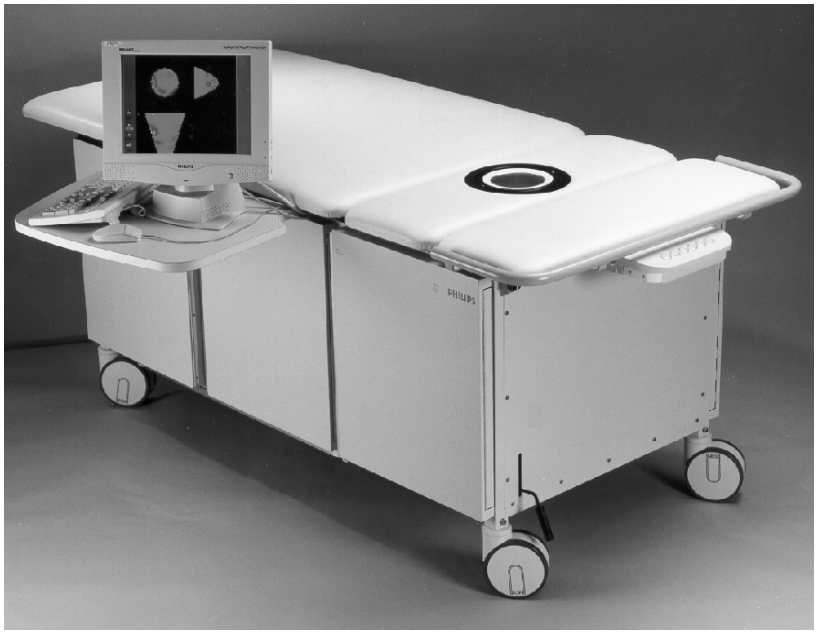

Figure 2-4. Prototype of a diffuse optical tomography system for breast imaging: The Philips 'Mammoscope'.

4.2 Photoacoustic tomography

Biomedical photoacoustic imaging is an imaging technique that is based on the generation of acoustic waves by pulsed light[43,44]. When a short laser pulse heats absorbers inside the tissue (like a specially designed agent), a temperature rise occurs, which is proportional to the deposited energy. As a result, a thermoelastic pressure transient is generated, whose amplitude depends on the amount of absorbed light, being determined by the local energy fluence, and the optical absorption coefficient of the target. From the

time this pressure wave needs to reach the tissue surface (detector position), the position of the photoacoustic source can be calculated when the speed of sound in tissue is known.

Photoacoustic tomography overcomes the resolution disadvantages of pure optical imaging, and the contrast and speckle disadvantages of pure Ultrasound imaging. As imaging agents, indocyanine dyes, with strong absorption in the near infrared spectra, are especially useful because of the relatively low absorption of NIR light in human tissue. For example, indocyanine green (ICG), which has been approved by the Food and Drug Administration, in combination with NIR techniques, is employed widely in clinical applications such as cardiac output monitoring, hepatic function study, and angiography in ophthalmology and tumor detection.

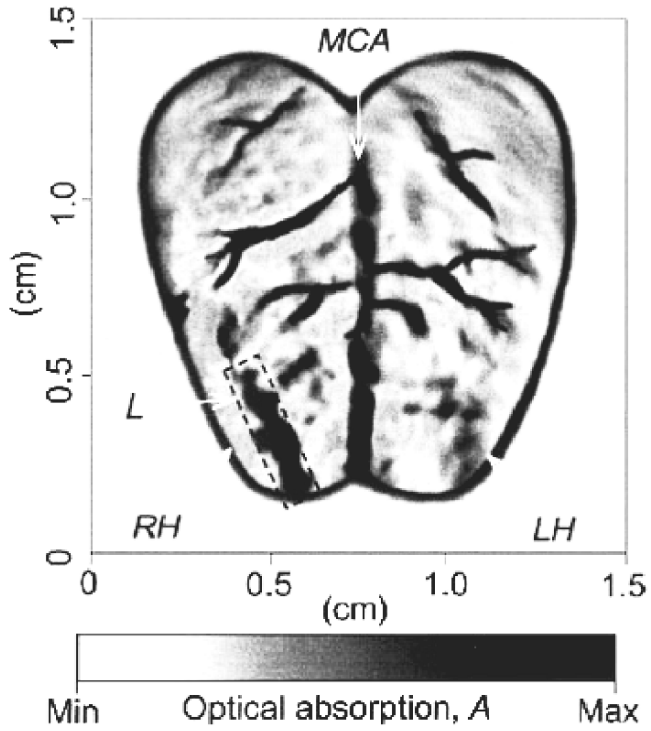

Figure 2-5. Non-invasive photoacoustic tomography image of a superficial lesion (size 1mm x 4mm) on a rat's cerebra, acquired with the skin and skull intact (taken from Wang et al.[45], image courtesy of Nature Publishing Group).

Current research on this technique focuses on animal experiments. Published results indicate that photoacoustic tomography is a noninvasive

means for localizing and quantifying regional brain hemodynamic responses to neural activities through the skin and skull with high optical contrast and high ultrasonic resolution in vivo[45] (see also Figure 2-5 for an example). Using multiple wavelengths, photoacoustic tomography should be able to visualize brain neoplasias and brain metastases from distant organs. Imaging of the human brain, although much more difficult, might be feasible.

4.3 Magnetic particle imaging

The use of magnetic particles like SPIOs (super-paramagnetic iron-oxide particles) for MR imaging is already well established in clinical practice. These particles modify the T1 and T2 relaxation times. However, the measurement of the concentration of the imaging agent is limited in sensitivity, since only changes in relaxation times are detected in the presence of a high background signal.

Magnetic Particle Imaging[46] follows a completely different approach. This technique takes advantage of the non-linear magnetization curve of the magnetic particles, and of the fact that the magnetization curve saturates at certain magnetic field strength. Figure 2-6 demonstrates the principle how to translate that into an imaging principle.

If an oscillating magnetic field is applied to a collection of magnetic particles, it will modulate the magnetization M of the magnetic material. The modulation of the magnetization will not only contain the drive frequency, but also a number of higher harmonics, which can easily be separated from the drive frequency.

The effect described above is most pronounced in the absence of any other field except the modulation field. However, if the magnetic particles are exposed to a time constant magnetic field with a sufficiently large magnitude (as shown in part b of Figure 2-6), they saturate and the generation of harmonics is suppressed.

The suppression of harmonics can now be used to perform a spatial encoding, which is a prerequisite for an imaging system. In addition to the modulation field, a time-independent field is superimposed, which vanishes in one point of the imaging device. If there is any magnetic material in the location of the field-free point, it will produce a signal containing higher harmonics. All other material outside the field-free point will remain in saturation. By steering the field-free point through the volume of interest, a tomographic image can be generated.

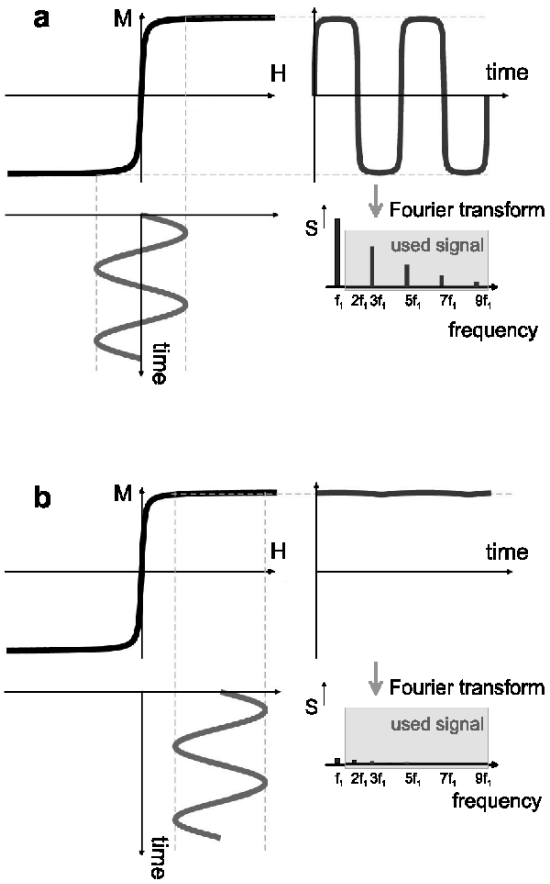

Figure 2-6. Response of magnetic particles to an external magnetic field. a) An oscillating magnetic field is applied to the magnetic material. As the magnetization curve (thick black curve) is nonlinear, the resulting time-dependent magnetization exhibits higher harmonics. b) A time-independent magnetic field is added to the modulation field. The oscillating field does not significantly change the magnetization of the material, as it is always in saturation (pictures courtesy of Nature Publishing Group).

REFERENCES

1. J.J. Wild, J.M. Reid, Echographic visualization of lesions of the living intact human breast, *Cancer Res* **14**, 277-283 (1954).
2. D.E. Kuhl, R.Q. Edwards, Image separation radioisotope scanning, *Radiology* **80**, 653-662(1963).

3. G.N. Hounsfield, Computerized transverse axial scanning (tomography). Part I: Description of system, *Br J Radiol* **46**, 1016-1022 (1974).
4. M.M. Ter-Pogossian, M.E. Phelps, E.J. Hoffman, N.A. Mullani, A positron-emission transaxial tomograph for nuclear imaging, *Radiology* **114**, 89-98 (1975).
5. P.C. Lauterbur, Image formation by induced local interactions: Examples employing nuclear magnetic resonance, *Nature* **242**, 190-191 (1973).
6. A.N. Garroway, P.K. Grannell, P. Mansfield, Image formation in NMR by a selective irradiative process, *J Phys, C: Solid State Phys* **7**, 457-462 (1974).
7. G.E. Moore, Cramming more components onto integrated circuits, *Electronics* **38**, 114-117 (1965).
8. M. Sonoda, M. Takano, J. Miyahara, H. Kato, Computed radiography utilizing scanning laser stimulated luminescence, *Radiology* **148**, 833-838 (1983).
9. J.A. Rowlands, The physics of computed radiography, *Phys Med Biol* **47**, R123-R166 (2002).
10. W. Zhao, I. Blevis, S. Germann, J.A. Rowlands, D. Waechter, Z. Huang, A flat panel detector for digital radiuology using active matrix readout of amorphous selenium, *The Physics of Medical Imaging*, *Proc SPIE* **2708**, 523-531 (1996).
11. A. Brauers, N. Conrads, G. Frings, U. Schiebel, M.J. Powell, C. Glasse, X-ray sensing properties of a lead oxide photoconductor combined with an amorphous silicon TFT array, *Mat Res Soc Symp Proc* **507**, 321-326 (1998).
12. L. E. Antonuk, J. Yorkston, W. Huang, J. Boudry, E. J. Morton, R. A. Street, Large area, flat-panel aSi:H arrays for x-ray imaging, *The Physics of Medical Imaging, Proc SPIE* **1896**, 18-29 (1993).
13. U. Schiebel, N. Conrads, N. Jung, M. Weibrecht, H. Wieczorek, T. Zaengel, M.J. Powell, I.D. French, C. Glasse, Fluoroscopic x-ray imaging with amorphous silicon thin-flim arrays, *The Physics of Medical Imaging, Proc. SPIE* **2163**, 129-140 (1994).
14. P.R. Granfors, D. Albagli, J.E. Tkaczyk, R. Aufrichtig, H. Netel, G. Brunst, J.M. Boudry, D. Luo, Performance of a flat-panel cardiac detector, *The Physics of Medical Imaging, Proc. SPIE* **4320**, 77-86 (2001).
15. F. Busse, W. Ruetten, B. Sandkamp, P.L. Alving, R.J. Bastiaens, T. Ducourant, Design and performance of a high-quality cardiac flat detector, *The Physics of Medical Imaging, Proc SPIE* **4682**, 819-827 (2002).
16. T. Graeve, G.P. Weckler, High-resolution CMOS imaging detector, *The Physics of Medical Imaging, Proc SPIE* **4320**, 68-76 (2001).
17. M. Schumacher, K. Kutluk, D. Ott, Digital rotational radiography in neuroradiology, *AJNR Am J Neuroradiol* **10**(3), 644-649 (1989).
18. A. Katsevich, A general scheme for constructing inversion algorithms for cone beam CT, *Int J Math Sci* **21**, 1305-1321 (2003).
19. H. Zaidi, M.-L. Montandon, The new challenges of brain PET imaging technology, *Curr Med Imag Rev* **2**, Bentham Science Publishers, in press (2006).

20. E.J. Hoffman, M.E. Phelps, N. Mullani, C.S. Higgins, B.E. Sobel, M.M. Ter-Pogossian, Design and performance characteristics of a whole-body transaxial tomograph, *J Nucl Med* **17**, 493-502 (1976).
21. C.J. Thompson, Y.L. Yamamoto, E. Meyer, Positome II: A high efficiency positron imaging device for dynamic brain studies, *IEEE Trans Nucl Sci* **26**, 583-589 (1979).
22. M.M. Ter-Pogossian, D.C. Ficke, J.T. Hood, M. Yamamoto, N.A. Mullani, PETT VI: A positron emission tomograph utilizing cesium fluoride scintillation detectors, *J Comput Assist Tomogr* **6**, 125-133 (1982).
23. T.R. deGrado, T.G. Turkington, J.J. Williams, C.W. Stearns, J.M. Hoffman, R.E. Coleman, Performance characteristics of a whole body PET scanner, *J Nucl Med* **35**, 1398-1406 (1994).
24. G. Muehllehner, J.S. Karp, S. Surti, Design considerations for PET scanners, *J Nucl Med* **46**, 16-23 (2002).
25. C.L. Melcher, Scintillation crystals for PET, *J Nucl Med* **41**, 1051-1055 (2000).
26. M.M. Ter-Pogossian, N.A. Mullani, D.C: Ficke, J. Markham, D.L. Snyder, Photon time-of-flight-assisted positron emission tomography, *J Comput Assist Tomogr* **5**, 227-239 (1981).
27. S. Surti, J.S. Karp, G. Muehllehner, Image quality assessment of LaBr3-based wholebody 3D PET scanners: A Monte Carlo evaluation, *Phys Med Biol* **49**, 4593-4610 (2004).
28. P. Dorenbos, Light output and energy resolution of Ce3+-doped scintillators, *Nucl Instr Meth A* **486**, 208-213 (2002).
29. A. Del Guerra, M.G. Bisogni, C. Damiani, G. Di Domenico, R. Marchesini, G. Zavattini, New developments in photodetection for medicine, *Nucl Instr Meth A* **442**, 18-25 (2000).
30. J.L. Humm, A. Rosenfeld, A. Del Guerra, From PET detectors to PET scanners, *Eur J Nucl Med* **30**, 1574-1597 (2003).
31. D. Renker, Properties of avalanche photodiodes for applications in high energy physics, astrophysics and medical imaging, *Nucl Instr Meth A* **486**, 164-169 (2002).
32. Y. Shao, R.W. Silverman, R. Farrell, I Cirignano, R. Grazioso, K.S. Shah, G. Visser, M. Clajus, T.O. Turner, S.R. Cherry, Design studies of a high resolution PET detector using APD arrays, *IEEE Trans Nucl Sci* **47**, 1051-1057 (2000).
33. H.O. Anger, A new instrument for mapping gamma-ray emitters, *Biology and Medicine Quarterly Report UCRL* **3653**, 38 (1957).
34. H.M. Hudson, R.S. Larkin, Accelerated image reconstruction unsing ordered subsets of projection data, *IEEE Trans Med Imag* **13**, 601-609 (1994).
35. G.L. Zeng, D. Gagnon, CdZnTe strip detector SPECT imaging with a slit collimator, *Phys Med Biol* **49**, 2257-2271 (2004).
36. D.B. Everett, J.S. Fleming, R.W. Todd, J.M. Nightingale, Gamma-radiation imaging system based on the Compton effect, *Proc Inst Electr Eng.* **124**, 995-1000 (1977).
37. K.P. Pruessmann, M. Weiger, M.B. Scheidegger, P. Boesiger, SENSE: Sensitivity encoding for fast MRI, *Magn Reson Med* **42**, 952-962 (1999).

38. D.K. Sodickson, W.J. Manning, Simultaneous acquisition of spatial harmonics (SMASH): Fast imaging with radiofrequency coil arrays, *Magn Reson Med* **38**, 591-603 (1998).
39. U. Katscher, P. Boernert, C. Leussler, J.S. van den Brink, Transmit SENSE, *Magn Reson Med* **49**, 144-150 (2003).
40. A.G. Sorenson, F.S. Buonanno, R.G. Gonzalez, L.H. Schwamm, M.H. Lev, Hyperactue stroke: Evaluation with combined multisection diffusion-weighted and hemodynamically weighted echo-planar MR imaging, *Radiology* **199**, 391-401 (1996).
41. S.B. Colak, M.B. van der Mark, G.W. tHooft, J.H. Hoogenraad, E.S. van der Linden, F.A. Kuijpers, Clinical optical tomography and NIR spectroscopy for breast cancer detection, *IEEE J Quantum Electron* **5**, 1143-1158 (1999).
42. A.P. Gibson, J.C. Hebden, S.R. Arridge, Recent advances in diffuse optical imaging, *Phys Med Biol* **50**, R1-R43 (2005).
43. C.G.A. Hoelen, F.F.M. de Mul, R. Pongers, A. Dekker, Three-dimensional photoacoustic imaging of blood vessels in tissue, *Opt Lett* **23**, 648-650 (1998).
44. K.P. Kostli, D. Frauchiger, J.J. Niederhauser, G. Paltauf, H.P. Weber, M. Frenz, Optoacoustic imaging using a three-dimensional reconstruction algorithm, *IEEE J Sel Top Quant* **7**, 918-923 (2001).
45. X. Wang, Y. Pang, G. Ku, X. Xie, G. Stoica, L.V. Wang, Noninvasive laser-induced photoacoustic tomography for structural and functional in vivo imaging of the brain, *Nat Biotechnol* **21**, 803-806 (2003).
46. B. Gleich, J. Weizenecker, Tomographic imaging using nonlinear response of magnetic particles, *Nature* **435**, 1214-1217 (2005).